

RESEARCH PAPER



Knockdown of HNRNPM inhibits the progression of glioma through inducing ferroptosis

Jian Wang^{a#}, Xiaolin Luo^{b#}, and Dehua Liu^{c,d}

^aDepartment of Pathology, Ganzhou People's Hospital, Ganzhou, Jiangxi, China; ^bParty Committee Office, The Third Affiliated Hospital of Gannan Medical University/Affiliated stomatological hospital, Ganzhou, Jiangxi, China; ^cDepartment of Neurosurgery, First Affiliated Hospital of Gannan Medical University, Ganzhou, Jiangxi, China; ^dInstitute of Neurology, Gannan Medical University, Ganzhou, Jiangxi, China

ABSTRACT

Purpose: Ferroptosis acts as an important regulator in diverse human tumors, including the glioma. This study aimed to screen potential ferroptosis-related genes involved in the progression of glioma.

Materials and Methods: Differently expressed genes (DEGs) were screened based on GSE31262 and GSE12657 datasets, and ferroptosis-related genes were separated. Among the important hub genes in the protein-protein interaction networks, HNRNPM was selected as a research target. Following the knockdown of HNRNPM, the viability, migration, and invasion were detected by CCK8, wound healing, and transwell assays, respectively. The role of HNRNPM knockdown was also verified in a xenograft tumor model in mice. Immunohistochemistry detected the expression levels of HNRNPM and Ki67. Moreover, the ferroptosis was evaluated according to the levels of iron, glutathione peroxidase (GSH), and malondialdehyde (MDA), as well as the expression of PTGS2, GPX4, and FTH1.

Results: Total 41 overlapping DEGs relating with ferroptosis and glioma were screened, among which 4 up-regulated hub genes (HNRNPM, HNRNPA3, RUVBL1, and SNRPPF) were determined. The up-regulation of HNRNPM presented a certain predictive value for glioma. In addition, knockdown of HNRNPM inhibited the viability, migration, and invasion of glioma cells in vitro, and also the tumor growth in mice. Notably, knockdown of HNRNPM enhanced the ferroptosis in glioma cells. Furthermore, HNRNPM was positively associated with SMARCA4 in glioma.

Conclusions: Knockdown of HNRNPM inhibits the progression of glioma via inducing ferroptosis. HNRNPM is a promising molecular target for the treatment of glioma via inducing ferroptosis. We provided new insights of glioma progression and potential therapeutic guidance.

ARTICLE HISTORY

Received 22 February 2023

Revised 4 July 2023

Accepted 16 July 2023

KEYWORDS



Glioma; HNRNPM; ferroptosis; bioinformatics analysis; SMARCA4

Introduction


Glioma is a common kind of primary tumor in the central nervous system, accounting for approximately 80% intracranial malignant tumors [1]. Because glioma directly disturbs the brain function, it remains a severe threat to human's health, associating with a poor prognosis and high mortality [2]. Recent study has reported that oxidative stress is one of the key factors that disturb the balance of the brain and participates in the carcinogenic process of gliomas [3–5]. Similarly to other types of tumors, the surgery, chemotherapy, and radiotherapy are the conventional strategies for the treatment of glioma [1,6,7]. Not only that, antioxidants also have chemoprophylaxis, which

can delay the recurrence of glioma [8]. However, these strategies achieve limited improvements on the outcomes. Encouragingly, with the emerging of more and more molecular targets, molecular targeted therapy provides another attractive option for glioma [9,10]. Therefore, it is urgent to further elucidate the underlying mechanism of glioma and its potential targets.

Ferroptosis is a kind of iron-related programmed cell death, accompanied by iron accumulation and lipid peroxidation [11]. Ferroptosis is involved in the pathogenesis of various kinds of human diseases, such as ischemia-reperfusion injury, kidney injury, nervous system diseases, cardiovascular diseases, autoimmune diseases, and

CONTACT Dehua Liu  ldhwj@gmu.edu.cn  Department of Neurosurgery, First Affiliated Hospital of Gannan Medical University, No. 23, Qingnian Road, Zhanggong District, Ganzhou, Jiangxi 341000, China

[#]JianWang and Xiaolin Luo are Co-first authors.

 Supplemental data for this article can be accessed online at <https://doi.org/10.1080/15384101.2023.2286782>

tumors [11–14]. Notably, compared with normal cells, cancer cells require a larger supply of iron to achieve rapid proliferation [15–17]. Emerging studies have determined that ferroptosis acts a suppressor in tumor progression [18,19]. For example, dihydroartemisinin exerts an anti-tumor activity in glioma through inducing ferroptosis [20]. Both sevoflurane and apatinib can inhibit the viability of glioma cells through inducing ferroptosis [21,22]. High expression of GPX7 is associated with poor prognosis of glioma, and silencing of GPX7 promotes the oxidative stress associated with ferroptosis in glioma cells, while the loss of GPX7 makes gliomas sensitive to ferroptosis [23]. Similarly, the ferroptosis is also involved in the action mechanisms of many molecular targets in glioma, such as ACSL4 [24], SLC1A5 [25], miR-670-3p [26], OTUB1 [27], etc. Therefore, the induction of ferroptosis presents a great potential for glioma therapy.

High-throughput sequencing is a powerful tool to identify differently expressed genes (DEGs) in certain physiological and pathological status [28,29]. BUB1 is significantly overexpressed in glioma, and there is a significant relationship between BUB1 expression and poor prognosis in glioma patients [30]. Additionally, Circ0030018 is obviously overexpressed in glioma cell lines, and circ0030018 silencing can significantly inhibit the growth and invasion of glioma while promote the oxidative stress of glioma cells [31]. What's more, based on the gene expression profiles, various ferroptosis-related genes have been screened as potential biomarkers for glioma. Wan et al. have determined 19 ferroptosis-related genes are highly correlated with the progression of glioma in the aspects of grade, prognosis, drug resistance, autophagy, and migration [32]. Zheng et al. have identified 12 ferroptosis-related genes as prognostic markers for lower-grade glioma [33]. Previous studies have also determined that some of the DEGs screened by RNA-Seq are potential therapeutic targets for glioma. For example, circCDK14 functions an oncogene in promoting the malignant characteristics and blocking the ferroptosis in glioma cells [34]. CYP2E1 acts as an anti-oncogene in glioma via regulating the lipid metabolism and ferroptosis [35]. The ferroptosis mediated by CD44, HSPB1, and SLC40A1

contributes to the anti-tumor role of Acetaminophen in glioblastoma [36]. However, there are still many ferroptosis-related genes have not been revealed in glioma.

In this study, ferroptosis-related DEGs were screened based on microarray data. Following bioinformatic analysis, HNRNPM, an isolated hub gene caught our attention. HNRNPM is an important splicing factor that plays a crucial regulatory role in multiple malignancies, such as hepatocellular carcinoma [37], colorectal cancer [38], breast cancer [39], and prostate cancer [40]. However, the regulatory role of HNRNPM in the ferroptosis in glioma is rarely reported, which guides our subsequent researches. This study aimed to reveal potential molecular targets relating with ferroptosis for the treatment of glioma.

Material & methods

Microarray data and DEGs analysis

The data sets of GSE31262 and GSE12657 relating with glioma were selected from GEO database (<https://www.ncbi.nlm.nih.gov/geo/>). The microarray data were analyzed by GEO2R (www.ncbi.nlm.nih.gov/geo/geo2r), and the volcano plots were drawn. The box diagrams of cross comparability assessment were drawn by R package ggplot2. Specific probes met $p \leq 0.05$, and $|\log_{2}FC| > 2$ were considered as DEGs. Using the top 50 up-regulated and 50 down-regulated DEGs, a heat map was drawn by R package pheatmap referring to the fold change and corrected p-values.

Screening of ferroptosis-related DEGs

The DEGs related with ferroptosis were screened by Draw Venn Diagram based on the databases of GeneCards, BioGPS, and Genehopper, and a Venn diagram was drawn. The overlapping DEGs were selected for subsequent analysis.

Functional enrichment analysis

The isolated overlapping DEGs were functional enriched by Gene ontology (GO) and Kyoto Encyclopedia of Genes and Genomes (KEGG) analyses based on the Database for Annotation,

Visualization, and Integrated Discovery (<https://david.ncifcrf.gov/>). Relevant bar and bubble plots were drawn using an online software (<http://www.bioinformatics.com.cn/login/>)

Construction of protein-protein interaction (PPI) networks

Based on the isolated DEGs, PPIs were analyzed by STRING and those with comprehensive score > 0.4 were considered statistically significant. The PPI networks were visualized using Cytoscape, and the hub genes were screened using MCODE (a plugins of Cytoscape).

Go enrichment analysis of hub genes and expression prediction

A Go chord diagram was drawn to reveal the differences of isolated hub genes in biological functions via R package ggplot2. The expression of 4 hub genes (HNRNPM, HNRNPA3, RUVBL1, and SNRPPF) was analyzed based on the database of GEPIA (<http://gepia.cancer-pku.cn/index.html>).

Correlation analysis of tumor immune infiltration

ROC curve was established to reveal the predictive value of HNRNPM in glioma. The correlations of HNRNPM with CD8⁺ T cell immune infiltration were determined in different cancers via TIMER2.0. The correlation of HNRNPM with immune cell infiltration in glioma was analyzed by TIMER (<https://cistrome.shinyapps.io/timer/>).

Screening of HNRNPM-related genes

Potential genes that related with HNRNPM in glioma were screened based on the database of LinkedOmics (<http://www.linkedomics.org>). The correlation between HNRNPM and SMARCA4 expression was analyzed based on the database of GEPIA (<http://gepia.cancer-pku.cn/index.html>).

Cell culturing and transfection

A normal human nerve astrocyte line (HEB cells) and two glioma cell lines (U251 and LN229 cells) were purchased from the Guangzhou Institute of

Biomedicine and Health, Chinese Academy of Sciences (Guangzhou, China). All cells were maintained in DMEM supplemented with 10% FBS at 37°C with 5% CO₂.

Two small interfering RNAs targeting HNRNPM (si-HNRNPM-1 and -2), and non-targeting negative control (siNC) were synthesized by Ribobio (Guangzhou, China). Relevant sequences were listed in Table 1. The siRNAs were transfected into glioma cells using Lipo6000 (Beyotime, Shanghai, China) following the instructions. Some of the transfected cells were also treated with 10 μmol/L Fe-1 (an inhibitor of ferroptosis).

Tumor specimens

Human para-cancerous tissue (Control, *n* = 10) and glioma tumor tissue (Tumor tissue, *n* = 10) of glioma patients were collected, quickly snap-frozen in liquid nitrogen and reposit at -80°C for further experiment. The study protocol was approved by the ethics review board of First Affiliated Hospital of Gannan Medical University (Ethical number: LLSC-2023042801; Approval date: 23rd. Apr, 2023). We have obtained informed consent from all study individuals. All of the procedures were performed in accordance with the Declaration of Helsinki and relevant policies in China.

Table 1. The sequences of siRNAs and primers.

Names	Sequences (5'-3')
siNC-sense	UUCUCCGAACGUGUCACGUTT
siNC-antisense	ACGUGACACGUUCCGAGAATT
siRNA-1-sense	GGAUGUUAUAAAGAUUUUAAA
siRNA-1-antisense	UAAACAUCUUUAUACAUCAG
siRNA-2-sense	GGAAGAUGCUGAAAGGACAAU
siRNA-2-antisense	GGAAGAUGCUGAAAGGACAAU
GAPDH-F	CCGGGAACTGTGGCGTGATGG
GAPDH-R	AGGTGGAGGAGTGGGTGTCGCTGT
HNRNPM-F	GAGCGGAAGACCACTGAAAG
HNRNPM-R	TCATTTGGGATGTTGGGATT
RUVBL1-F	GCCAGCTAATGAAGCCAAAG
RUVBL1-R	GAAGCACTCAATGTCCAGCA
SNRPF-F	CAATCCCAAACCTTTCCTCA
SNRPF-R	CACCCAGATGTCCAGACAAA
HNRNPA3-F	AGACAGGCAGAGTGGGAAA
HNRNPA3-R	TTCTCCACGACCCATAAAG
SMARCA4-F	AGCGATGACGTCTCTGAGGT
SMARCA4-R	GTACAGGGACACCAGCCACT

Quantitative real-time PCR (qRT-PCR)

Total RNAs were extracted from cells using TRIzol (Beyotime) and immediately transcribed into cDNAs using Hiscript II qRT Supermix (Vazyme, Nanjing, China). qRT-PCR was run on 7300PLUS instrument (Applied Biosystems, Waltham, MA, USA) using SYBR Green qPCR Mix (Beyotime). Relative mRNA expression of target genes was calculated by the $2^{-\Delta\Delta Ct}$ method. GAPDH was used as an internal control, and the primer sequences were listed in Table 1.

Western blot

Cells or tissues were lysed in RIPA buffer (Beyotime) to isolate the total proteins. The protein samples were separated by 10% SDS-PAGE and transferred onto PDVF membranes (Millipore, Danvers, USA). Followed by 2 h of blocking with 5% nonfat milk, the membranes were incubated with primary antibodies (anti-HNRNPM, -PTGS2, -GPX4, -SLC7A11, and β -actin; Abcam, Cambridge, MA, USA) for 12 h at 4°C, and subsequent with secondary antibody (HRP-conjugated IgG, Abcam) for 2 h. The blots were finally visualized using ECL kit (Beyotime) and captured under an imaging system (Tanon 5200, Shanghai, China).

Cell counting kit-8 (CCK8) assay

The viability of U251/LN229 cells was measured using a CCK8 kit (Solarbio, Beijing, China). In brief, cells that seeded in 96-well plate (4×10^3 /well) were cultured for 24, 48, and 72 h, respectively. Subsequently, cells were incubated with CCK8 reagent for 2 h, and the optical density (OD) at 450 nm was then measured under a microplate reader (Multiskan SkyHigh, Thermo Fisher Scientific).

Wound healing assay

The migration of U251/LN229 cells was measured by wound healing assay. In brief, cells that seeded in 6-well plates (1×10^5 /well) were cultured until 80% confluence. A wound was then made along the diameter using pipette tips. After 3 times of

washing with PBS, cells were cultured in serum-free DMEM for 24 h. The wound distance was measured at 0 h and 24 h post-wounding, and the healing rate was finally calculated.

Transwell assay

The invasion of U251/LN229 cells was measured using Transwell chambers (Corning, Kennebunk, ME, USA). In brief, 5×10^4 cells were seeded into Matrigel-coated upper chamber, and DMEM containing 20% FBS was filled in the lower chamber. Followed by 24 h of culturing, cells in the lower chamber were collected for staining. Cells that stained with crystal violet were counted under microscope (Olympus).

Measurement of ferroptosis-related parameters

The content of cellular iron was measured using an Iron Assay Kit (Sigma, St. Louis, MO, USA) following the instructions. The contents of glutathione peroxidase (GSH) and malondialdehyde (MDA) in cell supernatants were measured using commercial enzyme-linked immunosorbent assay kits (Esebio, Shanghai, China) following the instructions. The mechanism diagram was plotted using the Figdraw website (www.figdraw.com).

Evaluation of tumor growth in a mouse model

A xenograft tumor model was established in BALB/c nude mice (4–5 weeks old, 18–20 g; Antaik, Beijing, China). In brief, U251 cells were transfected with recombinant lentivirus to stably knock down the expression of HNRNPM (LV-shHNRNPM, LV-shNC). Then, 3×10^6 transfected U251 cells were subcutaneously injected into mice at the right flank ($N = 6$ each group). The tumor volume was calculated according to the longest and shortest diameter every 7 days. After the last measurement at the 28th day, mice were anesthetized by intraperitoneal injection of pentobarbital sodium (50 mg/kg) and sacrificed by cervical dislocation. The separated tumor xenografts were weighed and used for western blot to detect the protein expression of HNRNPM and immunohistochemistry analysis. The above animal experiments were approved by the local ethical

committee following the Guide for the Care and Use of Laboratory Animals (Ethical number: 2022132; Approval date: 2nd. Mar, 2022).

Immunohistochemistry

Samples (xenograft-derived tumors, human para-cancerous tissue, and glioma tumor tissue) were fixed in 4% paraformaldehyde. After dehydration and hyalinization, the specimen was embedded in paraffin to prepare the sections for immunohistochemistry. The paraffin-embedded sections were dewaxed and rehydrated, and antigenic repair was performed with sodium citrate. Sections were incubated with 3% H₂O₂ at room temperature to quench endogenous peroxidase activity, and closed with BSA for 20 min. Then, primary antibodies (Anti-HNRNP, 1: 200, Abcam; Anti Ki67, 1:200, Abcam) were added to incubate the slides overnight at 4°C. The secondary antibody (1:1000, Abcam) was added for incubation for 1 h at 37°C. The immunohistochemical images were obtained with an optical microscope.

Statistical analysis

All data were presented as mean \pm standard deviation and were statistically analyzed by Prism 7.0 (GraphPad, San Diego, CA, USA). Comparisons between two groups were determined by *t* test. Comparisons among multiple groups were determined by One-way ANOVA and subsequent Tukey's test. $P < 0.05$ was regarded as statistically significant.

Result

Isolation of DEGs between glioma and normal samples

Based on the databases of GSE31262 and GSE12657, the DEGs in glioma samples were screened. Volcano plots showed massive up-regulated and down-regulated DEGs between the tumor and normal samples in these two data sets (Figure 1(a,b)). Cross comparability assessment revealed that the value distribution was standard,

indicating the microarray data have a high reliability and cross comparability (Figure 1(c,d)). Following the screening conditions of $p \leq 0.05$ and $|\log_2 \text{FC}| > 0.5$, total 3106 DEGs were isolated in GSE31262 and 3015 DEGs were isolated in GSE12657. Subsequently, total 726 overlapping DEGs were determined in both GSE31262 and GSE12657, among which 41 DEGs were isolated after intersected with ferroptosis (Figure 1(e)). The heat maps, including top 50 up-regulated and 50 down-regulated DEGs, shown in Figure 1(f,g). The top 10 up-regulated and 10 down-regulated DEGs in each database were listed in Table S1 and S2.

Functional enrichments of DEGs relating with glioma and ferroptosis

The isolated 41 DEGs relating with glioma and ferroptosis were functionally enriched. GO enrichment analysis revealed that the DEGs were mainly enriched in the biological processes (BP) of positive regulation of phosphorylation and cellular response to cadmium ion, cellular components (CC) of membrane raft and macromolecular complex, as well as molecular functions (MF) of enzyme binding and ubiquitin protein binding. The top six significantly enriched GO terms were listed in Figure 2(a,b). In addition, KEGG enrichment analysis showed that the DEGs were enriched in diverse signaling pathways, mainly including HIF-1 signaling pathway, ferroptosis, neurodegeneration, cancer, etc. The top 25 KEGG terms with minimum FDR were listed in Figure 2(c,d).

Screening of hub genes based on PPI network

PPI networks were established to screen key hub genes. As shown in Fig S1 A and C, two PPI networks were constructed using Cytoscape. After being screened by the connectivity ≥ 10 and maximum cluster centrality, two Hub gene modules were revealed, including module I composed by GASP8, EGFR, HIF1A, MAPK1, and NFKB1 (Fig S1B), as well as module II composed by HNRNPM, HNRNPA3, RUVBL1, and SNRPPF (Fig S1D). These hub genes were used for subsequent assays.

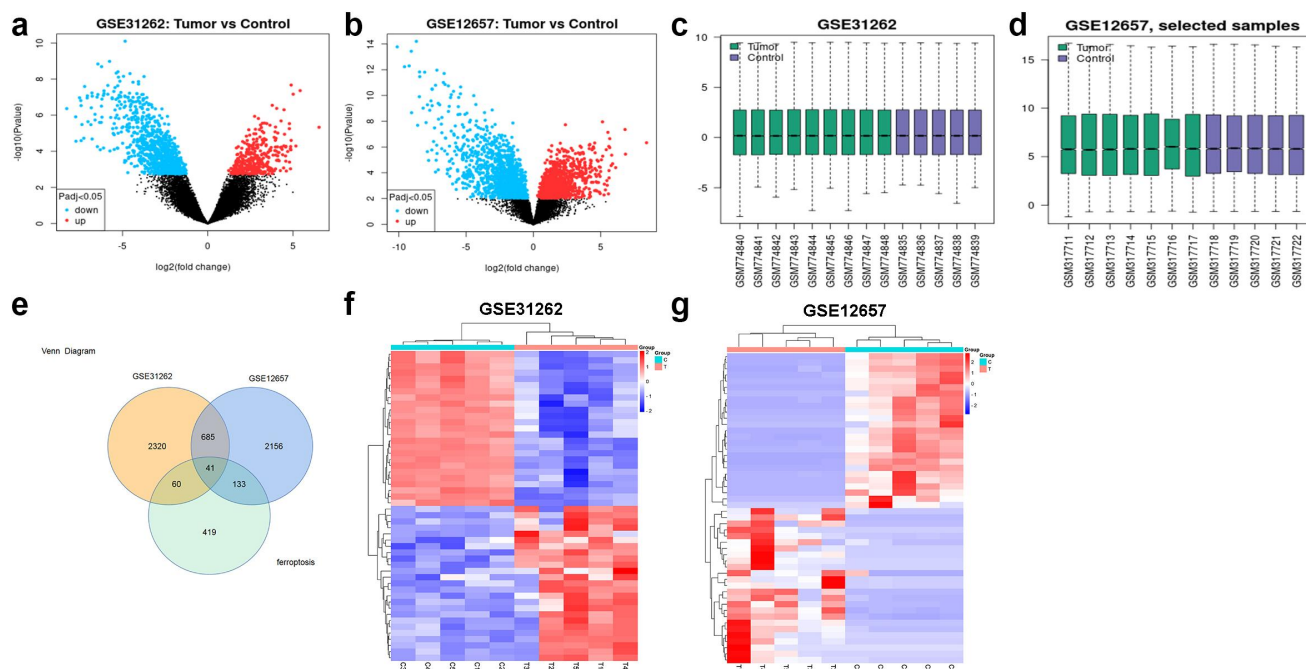


Figure 1. Screening of DEGs in glioma samples based on the database of GSE31262 and GSE12657. a-b, volcano plots of DEGs between the tumor and control samples; red dots represented the up-regulated DEGs, and the blue dots represented the down-regulated DEGs. c-d, cross comparability assessment of microarray data. e, isolation of overlapping DEGs associated with GSE31262, GSE12657, and ferroptosis. f-g, heat maps of DEGs between the tumor and control samples; red blocks represented the up-regulated DEGs, and the blue blocks represented the down-regulated DEGs.

Functional enrichments and expression of isolated hub genes

The isolated nine hub genes were further functionally enriched by GO analysis. The AGE/RAGE pathway, embryonic and placenta development, and complex spliceosome were mainly enriched by these hub genes (Fig S2A). Based on the database of GEPIA, the expression of these hub genes was analyzed. As presented in Fig S2B-E, the expression of HNRNPM, HNRNPA3, RUVBL1, and SNRPPF was significantly higher in tumor samples than that in the controls ($P < 0.05$).

HNRNPM is associated with tumor immune infiltration and tumor microenvironment

Among the isolated hub genes, HNRNPM caught our attention. ROC curve revealed that HNRNPM had a certain predictive value for glioma (AUC, 0.886) (Fig S3A). In addition, HNRNPM was associated with the immune infiltration of CD8⁺ T cells in diverse types of cancers, especially in head and neck squamous cell carcinoma (HNSC) and kidney renal clear cell carcinoma (KIRC).

Notably, HNRNPM was negatively associated with the immune infiltration of CD8⁺ T cells in glioblastoma (Fig S3B). In tumor microenvironment, HNRNPM was positively related with tumor purity, but not related with the immune infiltration of B cells, CD8⁺ T cells, CD4⁺ T cells, macrophages, neutrophils and dendritic cells (Fig S3C).

Expression validation of isolated hub genes

The expression of HNRNPM, HNRNPA3, RUVBL1, and SNRPPF was further verified in glioma cells. qRT-PCR determined that the mRNA expression of HNRNPM, HNRNPA3, RUVBL1, and SNRPPF was significantly higher in U251/LN229 cells than that in HEB cells (normal human nerve astrocytes) ($P < 0.05$, Figure 3(a)). The protein expression of HNRNPM (a target gene analyzed in this study) was also determined by western blot. In consistent with its mRNA expression, HNRNPM was up-regulated in U251/LN229 cells compared with that in HEB cells ($P < 0.05$, Figure 3(b)).

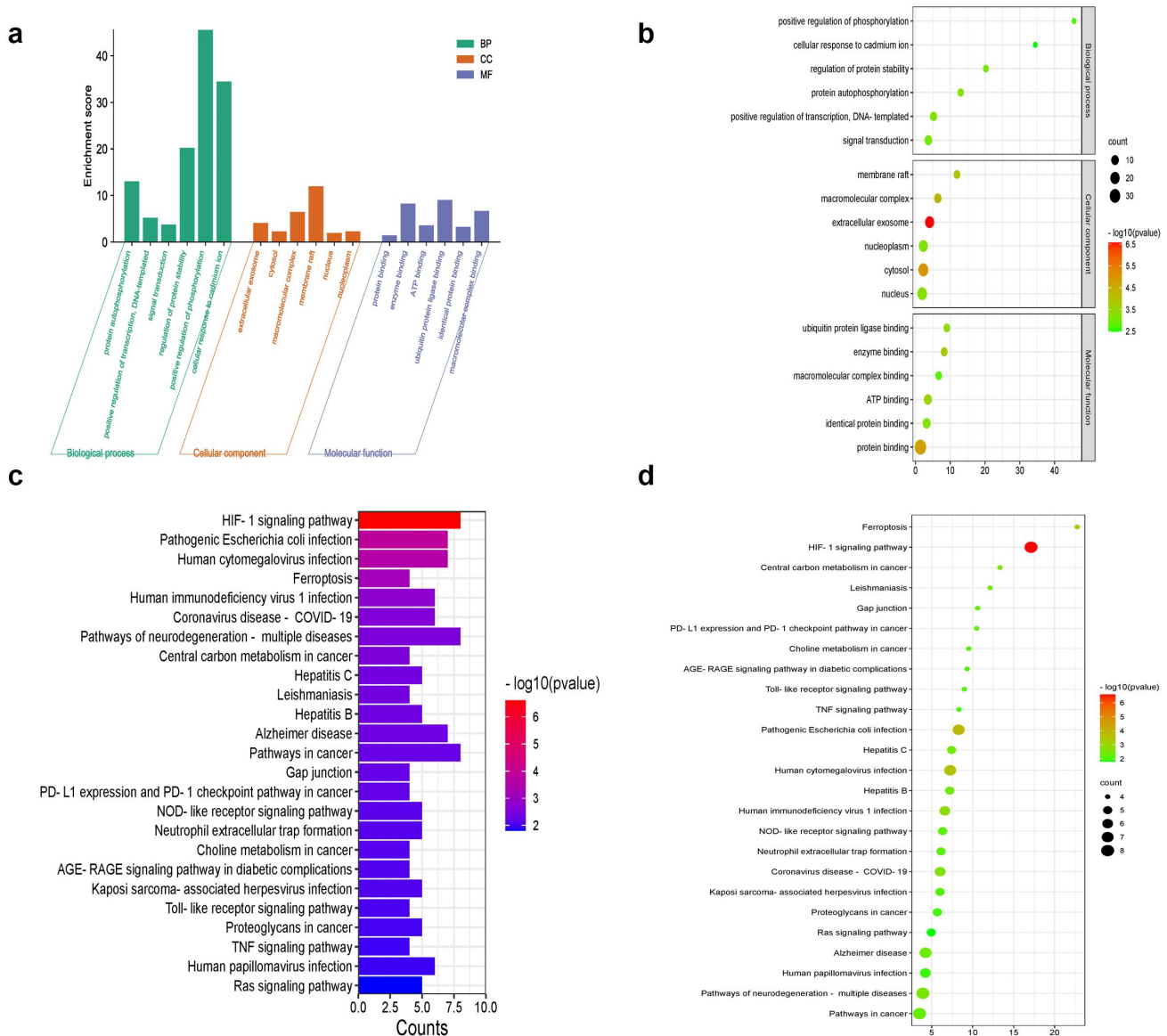


Figure 2. Functional enrichment of isolated DEGs. a, bar plots of GO enrichment analysis. b, bubble plots of GO enrichment analysis. c, bar plots of KEGG enrichment analysis. d, bubble plots of KEGG enrichment analysis.

Immunohistochemistry results further confirmed the result of western blot, which suggested that the expression level of HNRNPM was higher in tumor than in normal tissue (Figure 3(c)).

Knockdown of HNRNPM inhibits the viability, migration, and invasion of glioma cells

The function of HNRNPM was then evaluated in glioma cells following knockdown. qRT-PCR determined that HNRNPM was knocked down by the transfection of si-HNRNPM-1 and -2 in U251/LN229 cells ($P < 0.01$, Figure 4(a)). si-HNRNPM-2 with a relatively good knockdown

efficiency was used in functional assays (referred to as si-HNRNPM). As presented in Figure 4(b-d), the transfection of si-HNRNPM significantly decreased the viability, wound healing rate, and invasion rate of U251/LN229 cells ($P < 0.01$). These results indicated that the knockdown of HNRNPM inhibited the viability, migration, and invasion of glioma cells.

Knockdown of HNRNPM inhibits tumor growth in mice

To further reveal the function of HNRNPM *in vivo*, a xenograft tumor model was established

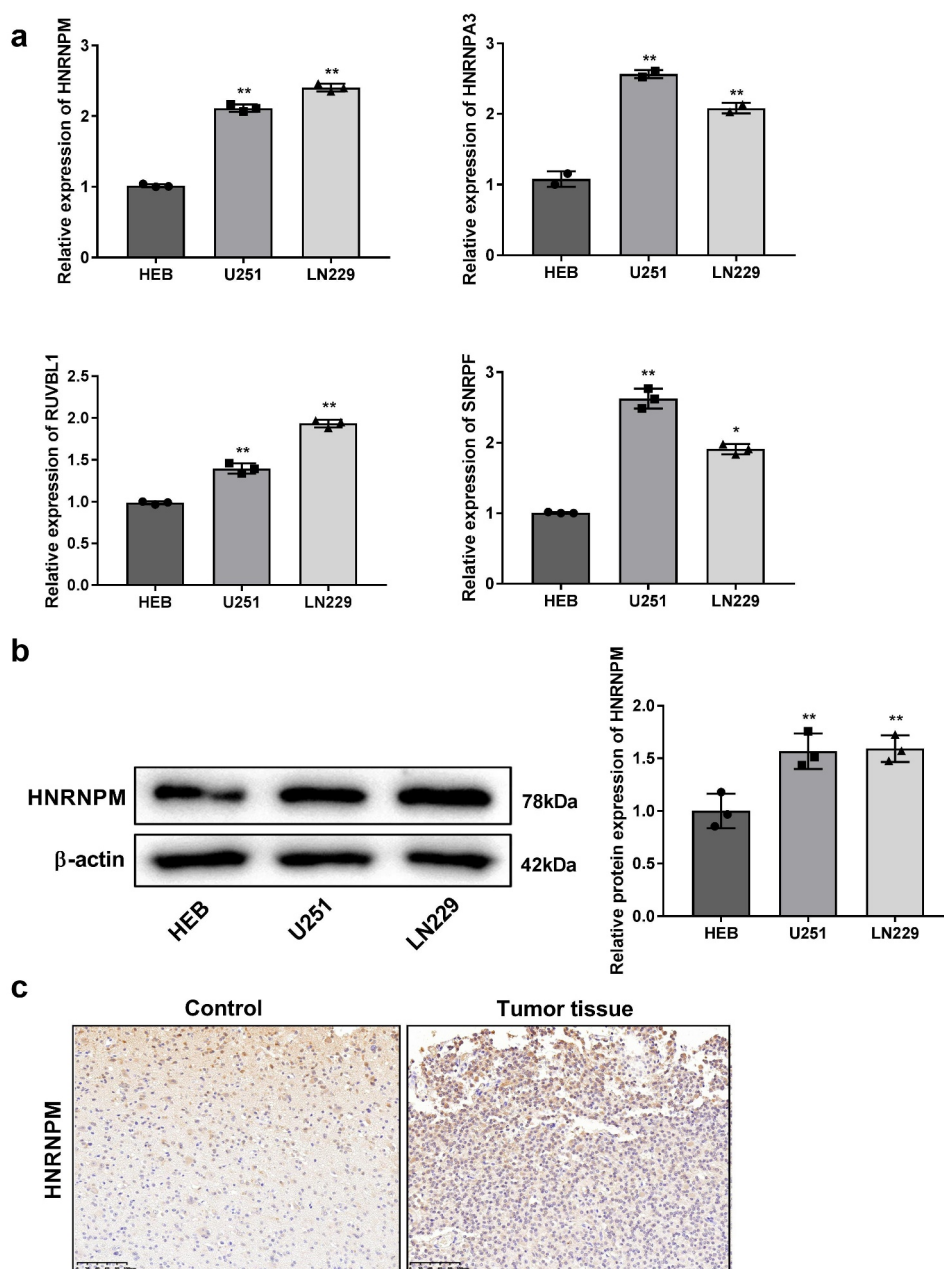


Figure 3. Validation of the expression of 4 hub genes. **a**, the mRNA expression of HNRNPM, HNRNPA3, RUVBL1, and SNRPPF was measured in glioma cells (U251/LN229 cells) and normal human nerve astrocytes (HEB cells) by qRT-PCR. **b**, the protein expression of HNRNPM was measured in U251/LN229 cells and HEB cells by western blot. * $P < 0.05$, ** $P < 0.01$ vs. HEB cells. **c**, the expression level of HNRNPM was measured by immunohistochemistry (bar = 200 μm , 200 \times).

in mice. As shown in Figure 5(a–e), the expression level of HNRNPM in the LV-shHNRNPM group was lower than that in the LV-shNC group, and mice in the LV-shHNRNPM group presented significantly lower tumor volume and weight compared with mice in the LV-shNC group ($P < 0.01$).

In addition, the down-regulation of HNRNPM protein in tumor tissues of the LV-shHNRNPM group was verified by western blot ($P < 0.05$). In the LV-shHNRNPM group, the expression level of Ki67 was significantly decreased compared with the LV-shNC group (Figure 5(f)).

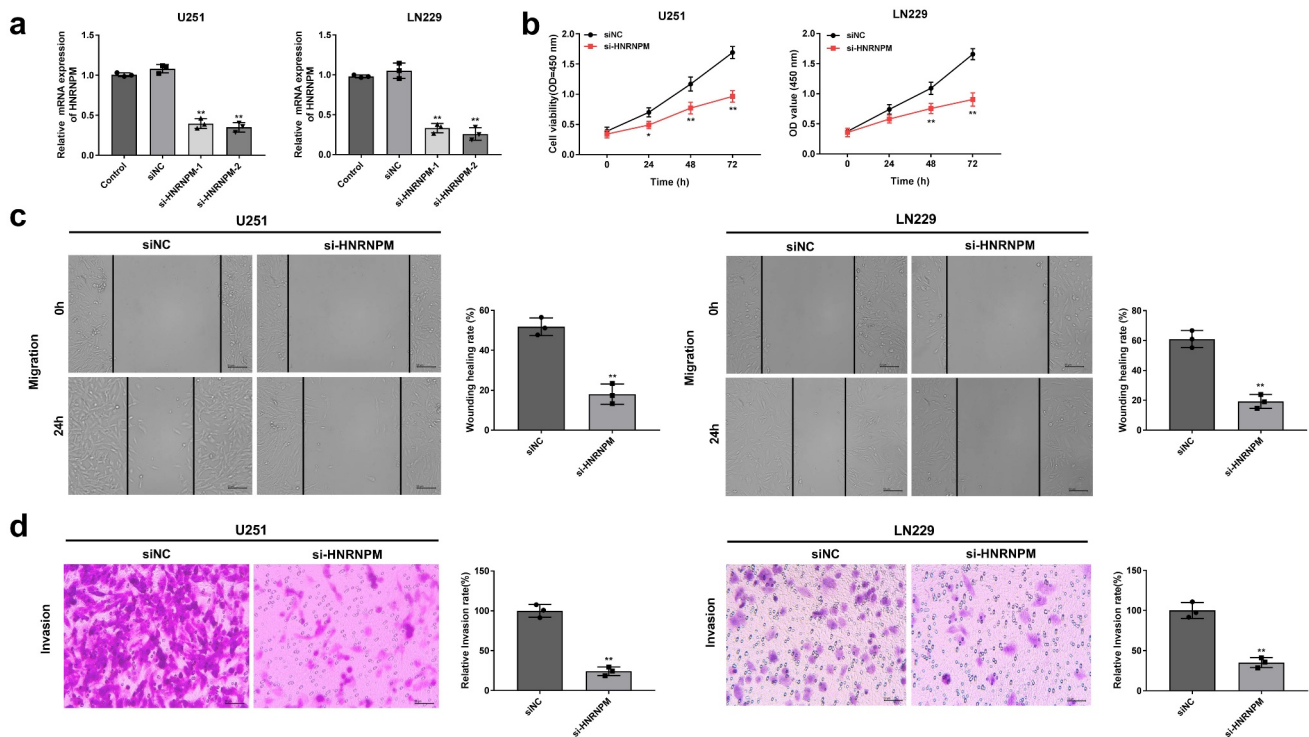


Figure 4. Knockdown of HNRNPM inhibits the viability, migration, and invasion of glioma cells. A, the knockdown efficiency of si-HNRNPM-1 and -2 in U251/LN229 cells was detected by qRT-PCR. B, the viability of U251/LN229 cells was measured by CCK8 assay. C, the migration of U251/LN229 cells was measured by wound healing assay. D, the invasion of U251/LN229 cells was measured by Transwell assay. ** $p < 0.01$ vs. siNC.

Knockdown of HNRNPM inhibits glioma progression via inducing ferroptosis

The regulatory role of HNRNPM in ferroptosis was analyzed in glioma cells. Compared with siNC-transfected cells, si-HNRNPM-transfected U251/LN229 cells exhibited significantly higher iron and MDA levels, and lower GSH level ($P < 0.01$, Figure 6(a-c)). The transfection of si-HNRNPM also significantly increased the protein expression of PTGS2 and decreased the protein expression of GPX4 and SLC7A11 in U251/LN229 cells ($P < 0.05$, Figure 6(d)). In addition, Fer-1, an inhibitor of ferroptosis significantly weakened the promoting effect of HNRNPM knockdown on ferroptosis, evidenced by decreased iron and MDA levels, increased GSH level, down-regulated PTGS2, and up-regulated GPX4 and SLC7A11 ($P < 0.05$, Figure 6(a-d)). The addition of Fer-1 had no significant effect on the viability, migration, and invasion of U251 cells, compared with the siNC group. Knockdown of HNRNPM

significantly suppressed the cell viability, migration, and invasion ($P < 0.01$), while Fer-1 reversed the inhibitory effect of knockdown HNRNPM on cell viability, migration, and invasion (Figure 7(a-c)). The mechanism diagram of HNRNPM regulating glioma via inducing ferroptosis was shown in Figure 7(d).

HNRNPM is positively associated with SMARCA4 in glioma

The correlations between HNRNPM and other genes were further analyzed. Based on the Linkedomics database, SMARCA4 was determined to be the top second gene that strongly correlated with HNRNPM (Figure 8(a,b)). A positive correlation between the expression of HNRNPM and SMARCA4 was determined in 125 glioma samples ($P < 0.001$, Figure 8(c)), and this correlation was also determined based on the database of GEPIA ($P < 0.001$, Figure 8(d)). In consistent with HNRNPM,

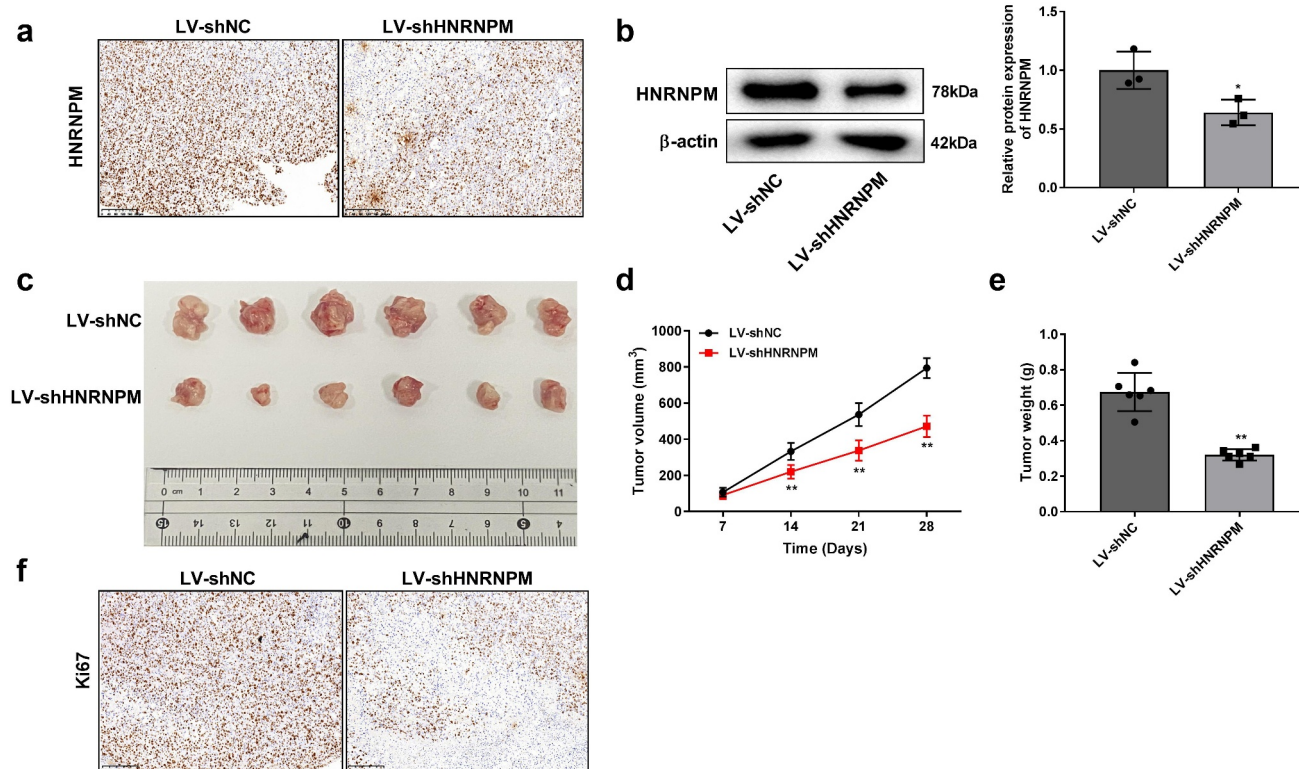


Figure 5. Knockdown of HNRNPM inhibits the growth of tumor xenografts in mice. a, the expression level of HNRNPM detected by immunohistochemistry. b, the protein expression of HNRNPM in xenograft tumors. c, tumor morphology. d, tumor volume. e, tumor weight. f, the expression level of Ki67 detected by immunohistochemistry (bar = 200 μ m, 200 \times), * P < 0.05, ** P < 0.01 vs. siNC.

SMARCA4 was also found to be up-regulated in U251/LN229 cells than that in HEB cells by qRT-PCR (P < 0.05, Figure 8(e)).

Discussion

Glioma is a common intrinsic brain tumor accompanied by poor prognosis. With the development of high-throughput sequences, more and more potential biomarkers and therapeutic targets have been discovered in diverse types of tumors, including the glioma [28,29,41]. This study was the first to identify HNRNPM, ferroptosis-related gene, as a pathogenic gene and to document its role in the malignant progression as well as its potential regulatory mechanisms of glioma. In this study, total 726 overlapping DEGs were determined based on GSE31262 and GSE12657. Subsequently, 41 ferroptosis-related DEGs were further screened due to the crucial regulatory role of ferroptosis in tumorigenesis and progression. Following the

establishment of PPI networks, HNRNPM came into our sight as a hub gene.

hnRNPs are a class of RNA-binding proteins that function in transcript-specific packaging and alternative splicing of pre-mRNAs [42,43]. Evidence has determined the crucial regulatory roles of hnRNPs in various neurodegenerative diseases, such as amyotrophic lateral sclerosis, Alzheimer's disease, fronto-temporal lobe dementia, and pinal muscular atrophy [44]. Notably, hnRNPs also participate in the occurrence and progression of human cancers [45]. Some up-regulated hnRNPs have been recognized as potential biomarkers for specific cancers, such as hnRNPK for hepatocellular carcinoma [46], hnRNPA1 for colorectal cancer [47], and hnRNP-A2/B1 for breast cancer [48]. In this study, HNRNPM, a member of hnRNP family was explored in glioma. In consistent with these hnRNPs mentioned above, the up-regulation of HNRNPM in glioma also exhibited a good

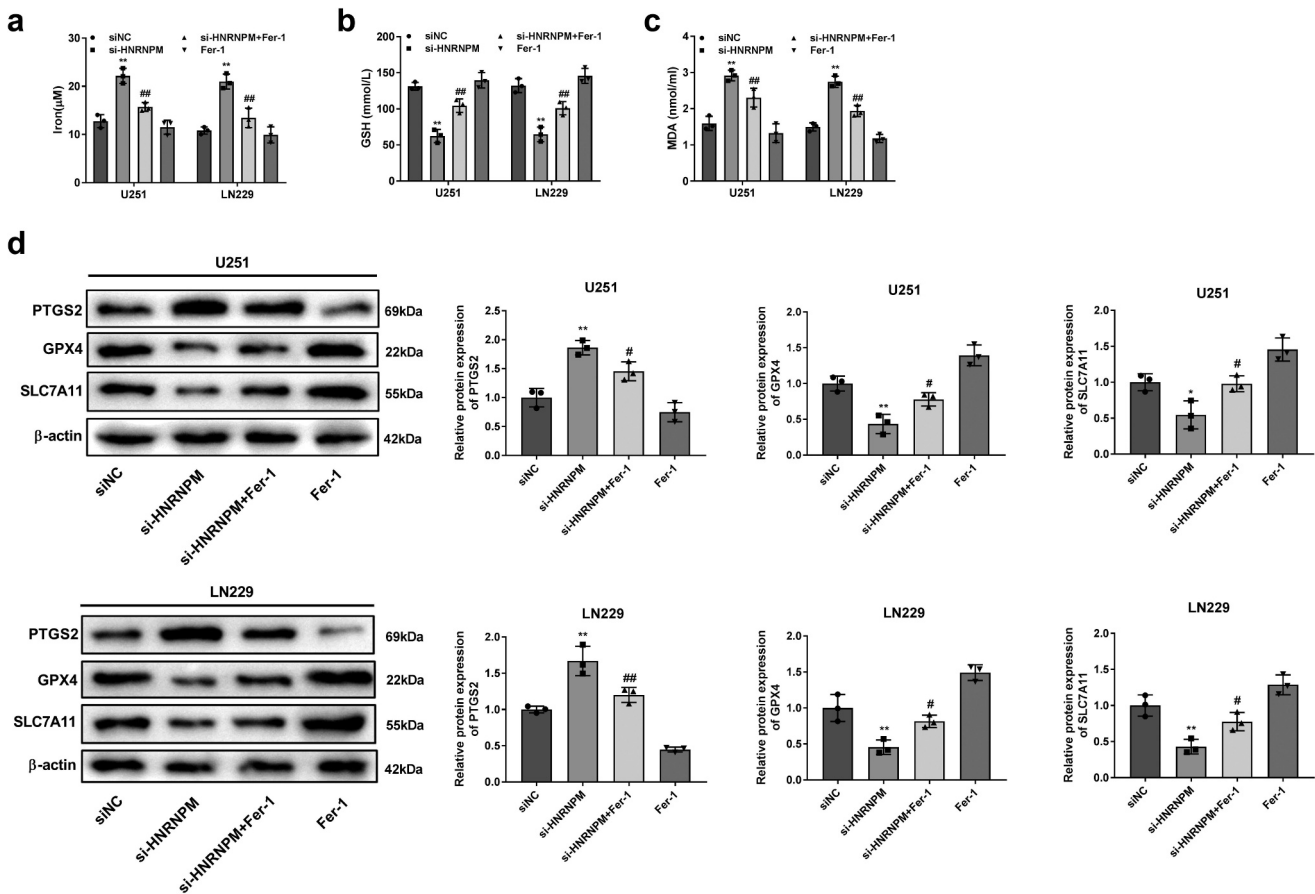


Figure 6. Knockdown of HNRNPM promoted the ferroptosis of glioma cells. a, the iron level. b, the GSH level. c, the ROS level. d, the protein expression of PTGS2, GPX4, and FTH1 (ferroptosis-related proteins) in U251/LN229 cells was measured by western blot. * $P < 0.05$, ** $P < 0.01$ vs. siNC; # $P < 0.05$, ## $P < 0.01$ vs. si-HNRNPM.

predictive value for glioma, indicating that HNRNPM may be a potential biomarker for glioma. In addition, HNRNPM has been reported to act as an oncogene in many cancers. Qiao et al. have shown that down-regulation of HNRNPM blocks the proliferation, migration, and epithelial mesenchymal transition of hepatocellular carcinoma cells [49]. Sun et al. have found that up-regulation of HNRNPM enhances the aggressiveness of breast cancer, associating with a poor prognosis in patients with lymph node metastasis [50]. Wang et al. have revealed that down-regulation of HNRNPM impairs the migration and invasion of gastric cancer cells [51]. However, research on the function of HNRNPM in glioma is still limited. Similarly with previous findings, this study discovered that knockdown of HNRNPM inhibited the viability, migration, and invasion of glioma cells.

Moreover, knockdown of HNRNPM could also inhibit the growth of tumor xenografts in mice. Our results indicated that HNRNPM might be a therapeutic target for glioma. Besides, a recent study has reported that the down-regulation of HNRNPM enhances anti-PD1 immunotherapy through promoting the infiltration of CD8⁺ T cells [37]. Here, a negative correlation of HNRNPM with the immune infiltration of CD8⁺ T cells was identified in glioblastoma. Therefore, HNRNPM may exert a tumor-intrinsic function in generating an immunosuppressive environment.

Until now, many molecules have been revealed as potential targets for glioma through regulating ferroptosis, such as ACSL4 [24], SLC1A5 [25], miR-670-3p [26], OTUB1 [27], etc. Some hnRNPs also participate in the regulation of ferroptosis in cancers. For example, overexpression of

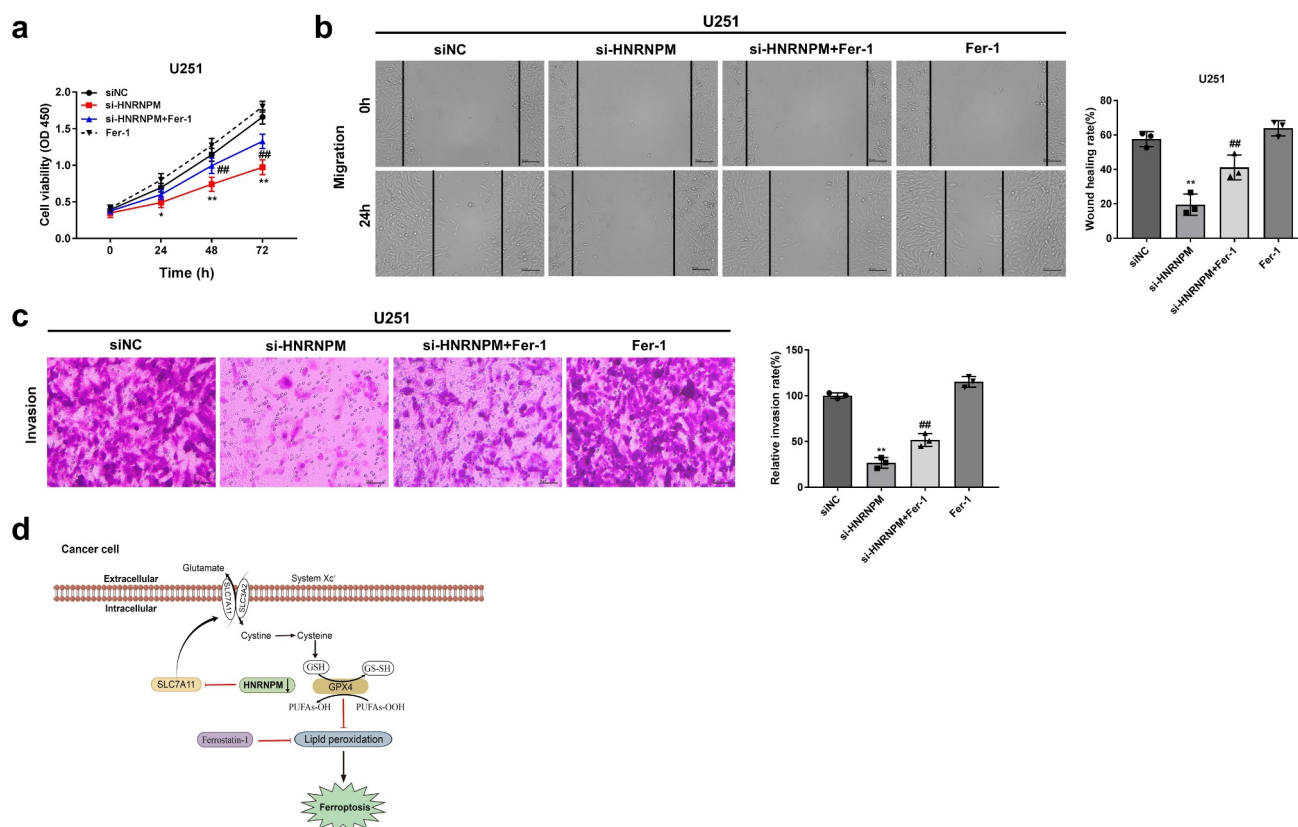


Figure 7. The effect of Fer-1 on glioma. **a**, the viability of U251 cells was measured by CCK8 assay. **b**, the migration of U251 cells was measured by wound healing assay. **c**, the invasion of U251 cells was measured by Transwell assay. **d**, the mechanism diagram of HNRNPM regulating glioma via ferroptosis. $**P < 0.01$ vs. siNC, $###P < 0.01$ vs. si-HNRNPM.

hnRNPL enhances the immune escape of castration-resistant prostate cancer cells through inhibiting ferroptosis, and down-regulation of hnRNPL can enhance the efficacy of anti-PD-1 therapy [52]. The degradation of hnRNPC mediated by CUL9 blocks erastin-induced ferroptosis in colorectal cancer, contributing to drug-resistant [53]. hnRNPA1-mediated packing of miR-522 in exosomes inhibits the ferroptosis in gastric cancer cells via blocking lipid-ROS accumulation [54]. However, the regulatory relationship between HNRNPM and ferroptosis is rarely reported in glioma. Here, knockdown of HNRNPM significantly increased iron and MDA levels, decreased GSH level, up-regulated PTGS2, and down-regulated GPX4 and SLC7A11 in glioma cells. And the above effects were reversed by the intervention of Fer-1. These results illustrate that knockdown of HNRNPM enhances the ferroptosis in glioma cells. Since induction of ferroptosis is

beneficial to inhibit tumor progression [18,19], we speculate that knockdown of HNRNPM may inhibits the progression of glioma through inducing ferroptosis.

As an important splicing factor, HNRNPM can interact with a variety of genes, such as ESRP1 [55], AKAP8 [56], MATR3 [57], CDR1 [58], RBFOX2 [59], etc. To further determine the action mechanisms of HNRNPM in glioma, potential genes that correlated with HNRNPM were analyzed. Among the predicted genes, SMARCA4 was determined to be positively associated with SMARCA4 in glioma. SMARCA4, also named BRG1, is an important transcription regulator in chromatin structure remodeling [60]. Bai et al. have shown that SMARCA4 is up-regulated in glioma tissues, and its silencing inhibits the proliferation, migration, and invasion of glioma cells [61]. Wang et al. have revealed that BRG-1 promotes the invasion and migration, and inhibits the

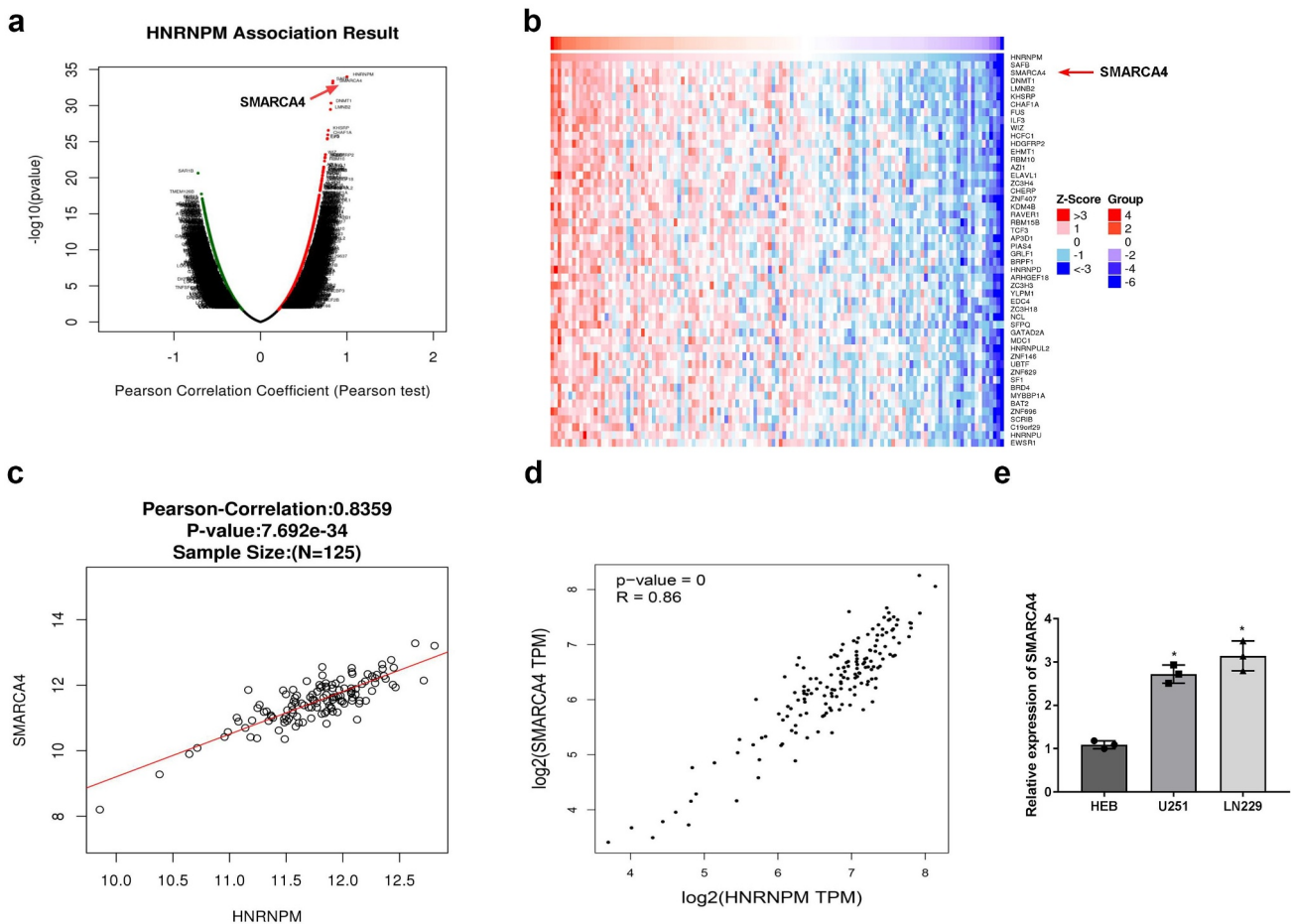


Figure 8. The isolation of potential genes correlated with HNRNPM. a, Pearson test; b, potential genes that positively correlated with HNRNPM were analyzed based on linkedomics database. c, the correlation between the expression of HNRNPM and SMARCA4 was determined in 125 glioma samples. d, the correlation between the expression of HNRNPM and SMARCA4 was determined based on GEPIA database. e, the mRNA expression of SMARCA4 was measured in U251/LN229 cells and HEB cells by qRT-PCR. * $P < 0.05$ vs. HEB cells.

chemotherapy sensitivity of glioblastoma cells [62]. Therefore, HNRNPM may be involved in the progression of glioma through interacting with SMARCA4.

Indeed, this study still presents some limitations. For example, the action mechanisms of HNRNPM involving SMARCA4 are not analyzed in depth. The roles of some other isolated hub genes in glioma are not explored. This study also lacks relevant validations based on clinical samples. Additionally, due to the limitations of laboratory conditions, the present study lacked the detection of lipid peroxides using BODIPY 581/591 C11 staining, an indicator for assessing ferroptosis. We will improve the laboratory equip-

ment and conditions to complete more experiments in the future research.

In conclusion, total 41 ferroptosis-related DEGs were screened in glioma. HNRNPM, a key hub gene was up-regulated in glioma, which was determined as a potential biomarker. Knockdown of HNRNPM inhibited the viability, migration, and invasion of glioma cells *in vitro*, as well as the tumor growth *in vivo*. Knockdown of HNRNPM also promoted the ferroptosis in glioma cells, which may contribute to the anti-tumor outcomes. In addition, there was a positive correlation between HNRNPM and SMARCA4 in glioma. Our findings indicate that HNRNPM may be a promising molecular target for the treatment of

glioma via inducing ferroptosis, which can provide new insights of glioma progression and potential therapeutic guidance for the follow-up targeted therapy of glioma.

Authors' contributions

Conceptualization: Jian Wang and Xiaolin Luo
 Formal analysis: Jian Wang, Xiaolin Luo and Dehua Liu
 Investigation: Jian Wang and Xiaolin Luo
 Methodology: Dehua Liu
 Writing – original draft: Jian Wang, Xiaolin Luo and Dehua Liu
 Writing – review & editing: Jian Wang and Xiaolin Luo
 Approval of final manuscript: all authors

Data availability statement

The datasets generated and/or analyzed during the current study are not publicly available due [Gannan Medical University] but are available from the corresponding author on reasonable request

Disclosure statement

No potential conflict of interest was reported by the authors.

Funding

The author(s) reported there is no funding associated with the work featured in this article.

Ethics approval and consent to participate

All experimental protocols were approved by the Animal Ethics Committee of Gannan Medical University.

All methods were carried out in accordance with the Guide for the Care and Use of Laboratory Animals.

All methods are reported in accordance with ARRIVE guidelines for the reporting of animal experiments. The study was carried out in accordance with the relevant guidelines and regulation.

References

- [1] Li J, Meng Q, Zhou X, et al. Gospel of malignant glioma: Oncolytic virus therapy. *Gene*. 2022;818:146217. doi: [10.1016/j.gene.2022.146217](https://doi.org/10.1016/j.gene.2022.146217)
- [2] Xue T, Ding JS, Li B, et al. A narrative review of adjuvant therapy for glioma: hyperbaric oxygen therapy. *Med Gas Res*. 2021;11(4):155–157. doi: [10.4103/2045-9912.318861](https://doi.org/10.4103/2045-9912.318861)
- [3] Borković-Mitić S, Stojsavljević A, Vujotić L, et al. Differences between antioxidant defense parameters and specific trace element concentrations in healthy, benign, and malignant brain tissues. *Sci Rep*. 2021;11(1):14766. doi: [10.1038/s41598-021-94302-5](https://doi.org/10.1038/s41598-021-94302-5)
- [4] Ramírez-Expósito MJ, Martínez-Martos JM. The delicate equilibrium between oxidants and antioxidants in brain glioma. *Curr Neuropharmacol*. 2019;17(4):342–351. doi: [10.2174/1570159X16666180302120925](https://doi.org/10.2174/1570159X16666180302120925)
- [5] Chen R, Lai UH, Zhu L, et al. Reactive oxygen species formation in the brain at different oxygen levels: the role of hypoxia inducible factors. *Front Cell Dev Biol*. 2018;6:132. doi: [10.3389/fcell.2018.00132](https://doi.org/10.3389/fcell.2018.00132)
- [6] Xu S, Tang L, Li X, et al. Immunotherapy for glioma: Current management and future application. *Cancer Lett*. 2020;476:1–12. doi: [10.1016/j.canlet.2020.02.002](https://doi.org/10.1016/j.canlet.2020.02.002)
- [7] Lim M, Xia Y, Bettegowda C, et al. Current state of immunotherapy for glioblastoma. *Nat Rev Clin Oncol*. 2018;15(7):422–442. doi: [10.1038/s41571-018-0003-5](https://doi.org/10.1038/s41571-018-0003-5)
- [8] Qi X, Jha SK, Jha NK, et al. Antioxidants in brain tumors: current therapeutic significance and future prospects. *Mol Cancer*. 2022;21(1):204. doi: [10.1186/s12943-022-01668-9](https://doi.org/10.1186/s12943-022-01668-9)
- [9] Yang K, Wu Z, Zhang H, et al. Glioma targeted therapy: insight into future of molecular approaches. *Mol Cancer*. 2022;21(1):39. doi: [10.1186/s12943-022-01513-z](https://doi.org/10.1186/s12943-022-01513-z)
- [10] Le Rhun E, Preusser M, Roth P, et al. Molecular targeted therapy of glioblastoma. *Cancer Treat Rev*. 2019;80:101896. doi: [10.1016/j.ctrv.2019.101896](https://doi.org/10.1016/j.ctrv.2019.101896)
- [11] Li J, Cao F, Yin HL, et al. Ferroptosis: past, present and future. *Cell Death Dis*. 2020;11(2):88. doi: [10.1038/s41419-020-2298-2](https://doi.org/10.1038/s41419-020-2298-2)
- [12] Wei X, Yi X, Zhu XH, et al. Posttranslational Modifications in Ferroptosis. *Oxid Med Cell Longev*. 2020;2020:1–12. doi: [10.1155/2020/8832043](https://doi.org/10.1155/2020/8832043)
- [13] Lai B, Wu CH, Wu CY, et al. Ferroptosis and Autoimmune Diseases. *Front Immunol*. 2022;13:916664. doi: [10.3389/fimmu.2022.916664](https://doi.org/10.3389/fimmu.2022.916664)
- [14] Wu X, Li Y, Zhang S, et al. Ferroptosis as a novel therapeutic target for cardiovascular disease. *Theranostics*. 2021;11(7):3052–3059. doi: [10.7150/thno.54113](https://doi.org/10.7150/thno.54113)
- [15] Lelièvre P, Sancey L, Coll JL, et al. Iron dysregulation in human cancer: altered metabolism, biomarkers for diagnosis, prognosis, monitoring and rationale for therapy. *Cancers (Basel)*. 2020;12(12):3524.
- [16] Lin CC, Chi JT. Ferroptosis of epithelial ovarian cancer: genetic determinants and therapeutic potential. *Oncotarget*. 2020;11(39):3562–3570. doi: [10.18632/oncotarget.27749](https://doi.org/10.18632/oncotarget.27749)
- [17] Jiang L, Kon N, Li T, et al. Ferroptosis as a p53-mediated activity during tumour suppression. *Nature*. 2015;520(7545):57–62. doi: [10.1038/nature14344](https://doi.org/10.1038/nature14344)
- [18] Zhang C, Liu X, Jin S, et al. Ferroptosis in cancer therapy: a novel approach to reversing drug

- resistance. *Mol Cancer*. 2022;21(1):47. doi: [10.1186/s12943-022-01530-y](https://doi.org/10.1186/s12943-022-01530-y)
- [19] Mou Y, Wang J, Wu J, et al. Ferroptosis, a new form of cell death: opportunities and challenges in cancer. *J Hematol Oncol*. 2019;12(1):34. doi: [10.1186/s13045-019-0720-y](https://doi.org/10.1186/s13045-019-0720-y)
- [20] Yuan Z, Chen X, Yang W, et al. The anti-inflammatory effect of minocycline on endotoxin-induced uveitis and retinal inflammation in rats. *Mol Vis*. 2019;25:359–372.
- [21] Xia L, Gong M, Zou Y, et al. Apatinib Induces ferroptosis of glioma cells through modulation of the VEGFR2/Nrf2 pathway. *Oxid Med Cell Longev*. 2022;2022:1–15. doi: [10.1155/2022/9925919](https://doi.org/10.1155/2022/9925919)
- [22] Xu Y, Zhang N, Chen C, et al. Sevoflurane induces ferroptosis of glioma cells through activating the ATF4-CHAC1 pathway. *Front Oncol*. 2022;12:859621. doi: [10.3389/fonc.2022.859621](https://doi.org/10.3389/fonc.2022.859621)
- [23] Zhou Y, Wu H, Wang F, et al. GPX7 is targeted by miR-29b and GPX7 knockdown enhances ferroptosis induced by Erastin in glioma. *Front Oncol*. 2021;11:802124. doi: [10.3389/fonc.2021.802124](https://doi.org/10.3389/fonc.2021.802124)
- [24] Cheng J, Fan YQ, Liu BH, et al. ACSL4 suppresses glioma cells proliferation via activating ferroptosis. *Oncol Rep*. 2020;43:147–158. doi: [10.3892/or.2019.7419](https://doi.org/10.3892/or.2019.7419)
- [25] Han L, Zhou J, Li L, et al. SLC1A5 enhances malignant phenotypes through modulating ferroptosis status and immune microenvironment in glioma. *Cell Death Dis*. 2022;13(12):1071. doi: [10.1038/s41419-022-05526-w](https://doi.org/10.1038/s41419-022-05526-w)
- [26] Bao C, Zhang J, Xian SY, et al. MicroRNA-670-3p suppresses ferroptosis of human glioblastoma cells through targeting ACSL4. *Free Radic Res*. 2021;55:853–864. doi: [10.1080/10715762.2021.1962009](https://doi.org/10.1080/10715762.2021.1962009)
- [27] Zhao X, Zhou M, Yang Y, et al. The ubiquitin hydrolase OTUB1 promotes glioma cell stemness via suppressing ferroptosis through stabilizing SLC7A11 protein. *Bioengineered*. 2021;12(2):12636–12645. doi: [10.1080/21655979.2021.2011633](https://doi.org/10.1080/21655979.2021.2011633)
- [28] Stark R, Grzelak M, Hadfield J. RNA sequencing: the teenage years. *Nat Rev Genet*. 2019;20(11):631–656. doi: [10.1038/s41576-019-0150-2](https://doi.org/10.1038/s41576-019-0150-2)
- [29] McCombie WR, McPherson JD, Mardis ER. Next-generation sequencing technologies. *Cold Spring Harb Perspect Med*. 2019;9(11):a036798. doi: [10.1101/cshperspect.a036798](https://doi.org/10.1101/cshperspect.a036798)
- [30] Zhang J, Wei W, Zhong Q, et al. Budding uninhibited by benzimidazoles 1 promotes cell proliferation, invasion, and epithelial-mesenchymal transition via the Wnt/ β -catenin signaling in glioblastoma. *Heliyon*. 2023;9(6):e16996. doi: [10.1016/j.heliyon.2023.e16996](https://doi.org/10.1016/j.heliyon.2023.e16996)
- [31] Liu A, Jiang B, Song C, et al. Isoliquiritigenin inhibits circ0030018 to suppress glioma tumorigenesis via the miR-1236/HER2 signaling pathway. *MedComm*. 2020;4:e282. doi: [10.1002/mco2.282](https://doi.org/10.1002/mco2.282)
- [32] Liu HJ, Hu HM, Li GZ, et al. Ferroptosis-Related Gene Signature Predicts Glioma Cell Death and Glioma Patient Progression. *Front Cell Dev Biol*. 2020;8:538. doi: [10.3389/fcell.2020.00538](https://doi.org/10.3389/fcell.2020.00538)
- [33] Zheng Y, Ji Q, Xie L, et al. Ferroptosis-related gene signature as a prognostic marker for lower-grade gliomas. *J Cell Mol Med*. 2021;25(6):3080–3090. doi: [10.1111/jcmm.16368](https://doi.org/10.1111/jcmm.16368)
- [34] Chen S, Zhang Z, Zhang B, et al. CircCDK14 promotes tumor progression and resists ferroptosis in glioma by regulating PDGFRA. *Int J Biol Sci*. 2022;18(2):841–857. doi: [10.7150/ijbs.66114](https://doi.org/10.7150/ijbs.66114)
- [35] Ye L, Xu Y, Wang L, et al. Downregulation of CYP2E1 is associated with poor prognosis and tumor progression of gliomas. *Cancer Med*. 2021;10(22):8100–8113. doi: [10.1002/cam4.4320](https://doi.org/10.1002/cam4.4320)
- [36] Deng S, Zheng Y, Mo Y, et al. Ferroptosis suppressive genes correlate with immunosuppression in glioblastoma. *World Neurosurg*. 2021;152:e436–e48. doi: [10.1016/j.wneu.2021.05.098](https://doi.org/10.1016/j.wneu.2021.05.098)
- [37] Zhu GQ, Wang Y, Wang B, et al. Targeting HNRNPM Inhibits Cancer Stemness and Enhances Antitumor Immunity in Wnt-activated Hepatocellular Carcinoma. *Cell Mol Gastroenterol Hepatol*. 2022;13(5):1413–1447. doi: [10.1016/j.jcmgh.2022.02.006](https://doi.org/10.1016/j.jcmgh.2022.02.006)
- [38] Chen TM, Lai MC, Li YH, et al. hnRNPM induces translation switch under hypoxia to promote colon cancer development. *EBioMedicine*. 2019;41:299–309. doi: [10.1016/j.ebiom.2019.02.059](https://doi.org/10.1016/j.ebiom.2019.02.059)
- [39] Xu Y, Gao XD, Lee JH, et al. Cell type-restricted activity of hnRNPM promotes breast cancer metastasis via regulating alternative splicing. *Genes Dev*. 2014;28(11):1191–1203. doi: [10.1101/gad.241968.114](https://doi.org/10.1101/gad.241968.114)
- [40] Yang T, An Z, Zhang C, et al. hnRNPM, a potential mediator of YY1 in promoting the epithelial-mesenchymal transition of prostate cancer cells. *Prostate*. 2019;79:1199–1210. doi: [10.1002/pros.23790](https://doi.org/10.1002/pros.23790)
- [41] Hong M, Tao S, Zhang L, et al. RNA sequencing: new technologies and applications in cancer research. *J Hematol Oncol*. 2020;13(1):166. doi: [10.1186/s13045-020-01005-x](https://doi.org/10.1186/s13045-020-01005-x)
- [42] Datar KV, Dreyfuss G, Swanson MS. The human hnRNP M proteins: identification of a methionine/arginine-rich repeat motif in ribonucleoproteins. *Nucleic Acids Res*. 1993;21(3):439–446. doi: [10.1093/nar/21.3.439](https://doi.org/10.1093/nar/21.3.439)
- [43] Martinez-Contreras R, Cloutier P, Shkreta L, et al. hnRNP proteins and splicing control. *Adv Exp Med Biol*. 2007;623:123–147.
- [44] Geuens T, Bouhy D, Timmerman V. The hnRNP family: insights into their role in health and disease. *Hum Genet*. 2016;135(8):851–867. doi: [10.1007/s00439-016-1683-5](https://doi.org/10.1007/s00439-016-1683-5)
- [45] Kedzierska H, Piekliko-Witkowska A. Splicing factors of SR and hnRNP families as regulators of apoptosis in cancer. *Cancer Lett*. 2017;396:53–65. doi: [10.1016/j.canlet.2017.03.013](https://doi.org/10.1016/j.canlet.2017.03.013)
- [46] Guo Y, Zhao J, Bi J, et al. Heterogeneous nuclear ribonucleoprotein K (hnRNP K) is a tissue biomarker for detection of early hepatocellular carcinoma in

- patients with cirrhosis. *J Hematol Oncol.* 2012;5(1):37. doi: [10.1186/1756-8722-5-37](https://doi.org/10.1186/1756-8722-5-37)
- [47] Ma YL, Peng JY, Zhang P, et al. Heterogeneous nuclear ribonucleoprotein A1 is identified as a potential biomarker for colorectal cancer based on differential proteomics technology. *J Proteome Res.* 2009;8(10):4525–4535. doi: [10.1021/pr900365e](https://doi.org/10.1021/pr900365e)
- [48] Zhou J, Allred DC, Avis I, et al. Differential expression of the early lung cancer detection marker, heterogeneous nuclear ribonucleoprotein-A2/B1 (hnRNP-A2/B1) in normal breast and neoplastic breast cancer. *Breast Cancer Res Treat.* 2001;66(3):217–224. doi: [10.1023/A:1010631915831](https://doi.org/10.1023/A:1010631915831)
- [49] Qiao L, Xie N, Li Y, et al. Downregulation of HNRNPM inhibits cell proliferation and migration of hepatocellular carcinoma through MAPK/AKT signaling pathway. *Transl Cancer Res TCR.* 2022;11(7):2135–2144. doi: [10.21037/tcr-21-2484](https://doi.org/10.21037/tcr-21-2484)
- [50] Sun H, Liu T, Zhu D, et al. HnRNPM and CD44s expression affects tumor aggressiveness and predicts poor prognosis in breast cancer with axillary lymph node metastases. *Genes Chromosomes Cancer.* 2017;56(8):598–607. doi: [10.1002/gcc.22463](https://doi.org/10.1002/gcc.22463)
- [51] Wang X, Li J, Bian X, et al. CircURI1 interacts with hnRNPM to inhibit metastasis by modulating alternative splicing in gastric cancer. *Proc Natl Acad Sci U S A.* 2021;118(33):118. doi: [10.1073/pnas.2012881118](https://doi.org/10.1073/pnas.2012881118)
- [52] Zhou X, Zou L, Liao H, et al. Abrogation of HnRNP L enhances anti-PD-1 therapy efficacy via diminishing PD-L1 and promoting CD8(+) T cell-mediated ferroptosis in castration-resistant prostate cancer. *Acta Pharm Sin B.* 2022;12:692–707. doi: [10.1016/j.apsb.2021.07.016](https://doi.org/10.1016/j.apsb.2021.07.016)
- [53] Yang L, WenTao T, ZhiYuan Z, et al. Cullin-9/p53 mediates HNRNPC degradation to inhibit erastin-induced ferroptosis and is blocked by MDM2 inhibition in colorectal cancer. *Oncogene.* 2022;41(23):3210–3221. doi: [10.1038/s41388-022-02284-z](https://doi.org/10.1038/s41388-022-02284-z)
- [54] Zhang H, Deng T, Liu R, et al. CAF secreted miR-522 suppresses ferroptosis and promotes acquired chemo-resistance in gastric cancer. *Mol Cancer.* 2020;19(1):43. doi: [10.1186/s12943-020-01168-8](https://doi.org/10.1186/s12943-020-01168-8)
- [55] Harvey SE, Xu Y, Lin X, et al. Coregulation of alternative splicing by hnRNPM and ESRP1 during EMT. *RNA.* 2018;24(10):1326–1338. doi: [10.1261/rna.066712.118](https://doi.org/10.1261/rna.066712.118)
- [56] Hu X, Harvey SE, Zheng R, et al. The RNA-binding protein AKAP8 suppresses tumor metastasis by antagonizing EMT-associated alternative splicing. *Nat Commun.* 2020;11(1):486. doi: [10.1038/s41467-020-14304-1](https://doi.org/10.1038/s41467-020-14304-1)
- [57] Ramesh N, Kour S, Anderson EN, et al. RNA-recognition motif in matrin-3 mediates neurodegeneration through interaction with hnRNPM. *Acta Neuropathol Commun.* 2020;8(1):138. doi: [10.1186/s40478-020-01021-5](https://doi.org/10.1186/s40478-020-01021-5)
- [58] Gu X, Li X, Jin Y, et al. CDR1as regulated by hnRNPM maintains stemness of periodontal ligament stem cells via miR-7/KLF4. *J Cell Mol Med.* 2021;25(9):4501–4515. doi: [10.1111/jcmm.16541](https://doi.org/10.1111/jcmm.16541)
- [59] Zhou D, Couture S, Scott MS, et al. RBFOX2 alters splicing outcome in distinct binding modes with multiple protein partners. *Nucleic Acids Res.* 2021;49(14):8370–8383. doi: [10.1093/nar/gkab595](https://doi.org/10.1093/nar/gkab595)
- [60] Pyo JS, Son BK, Oh D, et al. BRG1 is correlated with poor prognosis in colorectal cancer. *Hum Pathol.* 2018;73:66–73. doi: [10.1016/j.humpath.2017.12.013](https://doi.org/10.1016/j.humpath.2017.12.013)
- [61] Bai J, Mei PJ, Liu H, et al. BRG1 expression is increased in human glioma and controls glioma cell proliferation, migration and invasion in vitro. *J Cancer Res Clin Oncol.* 2012;138(6):991–998. doi: [10.1007/s00432-012-1172-8](https://doi.org/10.1007/s00432-012-1172-8)
- [62] Wang Y, Yang CH, Schultz AP, et al. Brahma-related gene-1 (BRG1) promotes the malignant phenotype of glioblastoma cells. *J Cell Mol Med.* 2021;25(6):2956–2966. doi: [10.1111/jcmm.16330](https://doi.org/10.1111/jcmm.16330)